

SIIV - 5th International Congress - Sustainability of Road Infrastructures

A Unified Approach for the Prediction of Vibration Induced by Underground Metro

Vittorio Nicolosi^{a*}, Mauro D'Apuzzo^b, Elena Bogazzi^c,

^aUniversity of Rome "Tor Vergata", Via del Politecnico 1, Rome 01000, Italy

^bUniversity of Cassino and Southern Lazio, Via G.Di Biasio 43, Cassino (FR) 03043, Italy

^cEngineer, Rome 01000, Italy

Abstract

In this paper a methodological approach employing a mathematical model to evaluate the vibration level transmitted by railway traffic is proposed. The originality of the approach is related to the explicit coupling of a vibration generation model which is based on the dynamic interaction between the railway vehicle and the superstructure with a vibration propagation model that analyses the dynamic interaction between the railway superstructure and the underlying soil/structures. The vibration level provided by the prediction model has been compared with vibration measurements carried out on a test site located along Turin underground line.

© 2012 The Authors. Published by Elsevier Ltd. Selection and/or peer-review under responsibility of SIIV2012 Scientific Committee

Keywords: Type your keywords here, separated by semicolons ;

1. Introduction

Underground metro networks can provide an effective solution to transport demand problems within a sustainable development framework although they can be characterized by high environmental impact [1, 2, 3]. Railway induced ground-borne vibrations affect both surface and underground lines and are often claimed to be responsible for cosmetic damages and for nuisance in buildings nearby.

During the past decades several engineering solutions have been proposed in order to mitigate the environmental impact related to vibration level induced by railway traffic. Most of this countermeasures have been conceived with reference to the railway track by making use of ballastless or slab track layouts with elastomeric and vibration absorbing pad/mats.

An alternative way to tackle the problem is to develop vehicle-oriented solutions. In this connection, rubber-tired metro may represent an effective countermeasure. It has to be reminded that a rubber-tired metro is a rapid

* Corresponding author. Tel.: +39-06-72597075; fax: +39-06-72597075.

E-mail address: nicolosi@uniroma2.it

transit system that is based on a mix of road and rail technology. The vehicles are equipped with rubber tyres running on rolling pads inside guide bars for traction. In some systems, conventional steel wheels are also present for guidance purpose in case a tire fails.

Since the contact area between wheel and rail is much wider than conventional steel to steel contact, interaction forces are much more lower than those experienced in conventional railways and therefore vibration are likely to be greatly reduced. However, even for these systems, there is the need to develop prediction tools in order allow transport engineers to assess potential vibration impact and to analyse suitable mitigation solutions.

In this paper, a mathematical model for the assessment of vibration transmitted by underground railway traffic is presented.

The model can be split into due sub-models according to the usual phenomenological approach to the problem: the generation model analyzing the dynamic interaction between the rolling stock and the railway superstructure, and a propagation model describing the vibration transmission through the tunnel lining and the surrounding soils. The novel feature of the model is to allow the coupling between the two sub-models. The model main features and the case study where it has been calibrated are reported in the followings.

2. Description of Mathematical Model

The dynamic forces transmitted to the subgrade that are liable for the ground-borne vibration generation are usually calculated by means of mathematical models representing the dynamic behavior of the whole-vehicle superstructure excited by the irregularities of the track. Mathematical models employed can be grouped according to the specific component described in the followings:

- vehicle models,
- rail defects models,
- rail superstructure models,

Vehicle are usually described by means of lumped mass discrete models. Input parameter are the mass and inertia moments of the railway car, bogies and wheel axles and the stiffness and damping characteristics of primary and secondary suspensions systems connecting the wheel axle with the bogie and the bogie with the railway car respectively [4, 5, 6, 7]. Similarly to the road case, rail defects can be represented by a stationary and ergodic random processes and therefore by means of Power Spectral Density (PSD) functions of vertical and transversal displacements. Several rail way companies have developed and proposed their own PSD based models for rail defects in the technical literature [2, 4, 5, 6, 8]. Railway superstructures are usually described by continuous or discrete models. In the former case, single winkler beams on a continuous visco-elastic support or multiple winkler beams are used if, in this latter case, several deformation levels need to be introduced in the model itself [3, 4, 5, 6, 9]. Discrete rail models are often been proposed by several authors if discrete connection between the rail and the underlying sleeper needs to be explicitly modeled.

As far as the propagation of ground-borne vibration generated by railway traffic is concerned, mathematical models may vary from simple viscoelastic half space to layered half space for surface railway lines. In this connection, several analytical mathematical models have been proposed in order to derive the dynamic Frequency Response Functions expressed in terms of vertical displacement experienced by a specific point at the surface level as a function of a pulsating vertical force. As far as underground lines are concerned, the tunnel structures makes analytical modeling more complex and therefore Finite Element Method (FEM) based models or hybrid Finite Element Method/Boundary Element Method (FEM/BEM) based models are usually preferred in order to describe the vibration propagation phenomenon throughout the surrounding soils [7, 10, 11].

In order to evaluate vibration induced by railway traffic, a common approach is to solve the dynamic interaction between the vehicle and the superstructure and then to apply the vertical dynamic forces evaluated so far to a propagation models. However this procedure is not always correct since the dynamic response vehicle-superstructure-subgrade system should be examined as a whole. In the proposed mathematical model, the

dynamic interaction between the vehicle, the rail defects, the railway superstructures and the surroundings soils or structures are examined in a unique system.

As far as the mathematical description of the model is concerned, if the connection between the railway superstructures and the surrounding soils/structures is considered as discrete (i.e. acting in a finite amount points) the following interaction forces can be identified:

$$F_{wr} = K_H \cdot (y_w - y_p - y_r) \tag{1}$$

at the wheel-rail level, where: F_{wr} is the vertical interaction force at the wheel-rail level, K_H is the Hertzian Spring Stiffness, y_w is the vertical displacement of the wheel, y_p is the vertical displacement of rail defects, y_r is the vertical displacement of the rail, and:

$$F_{rs} = (K_R + j \cdot \omega \cdot C_R) \cdot (y_r - y_s) \tag{2}$$

at the rail-soil/structure level, where: F_{rs} is the vertical interaction force rail-soil/structure level, K_R is the Elastic Stiffness of the Rail pad or of the rail support, C_R is the Damping Coefficient of the Rail pad or of the rail support, j is the imaginary unit, ω is the circular frequency, y_r is the vertical displacement of the rail, y_s is the vertical displacement of the soil/structure.

It is worth to be noticed that equation (1) can be written for each of the m contact points between the vehicle and the rail, whereas equation (2) can be written for each of the n contact points between the rail and the underlying soil/structure.

By applying a Fourier transform the aforementioned set of equations can be written in the frequency domain. For sake of clarity, the set of equation in the frequency domain is shown in the followings, assuming two contact points at the wheel rail interface and n contact points at the rail-soil/structure level:

$$\left\{ \begin{aligned} F_{w1r} &= K_H \cdot \left(H_{w11} \cdot F_{w1r} + H_{w12} \cdot F_{w2r} - Y_{p1} - H_{rw1w1} \cdot F_{w1r} - H_{rw1w2} \cdot F_{w2r} - \sum_{i=1}^n H_{rw1si} \cdot F_{rsi} \right) \\ F_{w2r} &= K_H \cdot \left(H_{w21} \cdot F_{w1r} + H_{w22} \cdot F_{w2r} - Y_{p1} \cdot e^{-j\omega L/V} - H_{r2w1} \cdot F_{w1r} - H_{r2w2} \cdot F_{w2r} - \sum_{i=1}^n H_{rw2si} \cdot F_{rsi} \right) \\ F_{rs1} &= (K_R + j \cdot \omega \cdot C_R) \cdot \left(H_{rs1w1} \cdot F_{w1r} + H_{rs1w2} \cdot F_{w2r} + \sum_{i=1}^n H_{rs1si} \cdot F_{rsi} - \sum_{i=1}^n H_{s1si} \cdot F_{rsi} \right) \\ &\dots\dots\dots \\ F_{rsn} &= (K_R + j \cdot \omega \cdot C_R) \cdot \left(H_{rsnw1} \cdot F_{w1r} + H_{rsnw2} \cdot F_{w2r} + \sum_{i=1}^n H_{rsnsi} \cdot F_{rsi} - \sum_{i=1}^n H_{snsi} \cdot F_{rsi} \right) \end{aligned} \right. \tag{3}$$

where:

- F_{w1r} is the vertical interaction force between the first wheel axle and the rail,
- F_{w2r} is the vertical interaction force between the second wheel axle and the rail,
- K_H is the Hertzian Spring Stiffness,
- H_{w11} is the Frequency Response Function (FRF) of the vertical displacement of the first vehicle wheel axle induced by a unit force applied on the first vehicle wheel axle,
- H_{w12} is the Frequency Response Function (FRF) of the vertical displacement of the first vehicle wheel axle induced by a unit force applied on the second wheel axle,
- H_{w21} is the Frequency Response Function (FRF) of the vertical displacement of the second vehicle wheel axle induced by a unit force applied on the first wheel axle,

H_{w22} is the Frequency Response Function (FRF) of the vertical displacement of the second vehicle wheel axle induced by a unit force applied on the second wheel axle,

Y_{p1} is the spectrum of rail defects experienced by the first wheel axle,

H_{rw1w1} is the Frequency Response Function (FRF) of the vertical displacement of the rail point under the first wheel axle induced by a unit force applied on the contact point between the first wheel axle and the rail,

H_{rw1w2} is the Frequency Response Function (FRF) of the vertical displacement of the rail point under the first wheel axle induced by a unit force applied on the contact point between the second wheel axle and the rail,

H_{rw1si} is the Frequency Response Function (FRF) of the vertical displacement of the rail point under the first wheel axle induced by a unit force applied on the i-contact point between the rail and the underlying soil/structure,

ω is the circular frequency,

L is the vehicle wheel base,

V is the train traveling speed,

F_{rs1} is the vertical interaction force in the first contact point between the rail and the underlying soil/structure,

F_{rsn} is the vertical interaction force in the n-contact point between the rail and the underlying soil/structure,

K_R is the Elastic Stiffness of the Rail pad or of the rail support,

C_R is the Damping Coefficient of the Rail pad or of the rail support,

j is the imaginary unit,

H_{rs1w1} is the Frequency Response Function (FRF) of the vertical displacement of the rail point located over the first contact point between the rail and the soil/structure, induced by a unit force applied on the contact point between the first wheel axle and the rail,

H_{rs1w2} is the Frequency Response Function (FRF) of the vertical displacement of the rail point located over the first contact point between the rail and the soil/structure, induced by a unit force applied on the contact point between the second wheel axle and the rail,

H_{rs1si} is the Frequency Response Function (FRF) of the vertical displacement of the rail point located over the first contact point connected to the soil/structure, induced by a unit force applied on the i-contact point between the rail and the soil/structure,

H_{s1si} is the Frequency Response Function (FRF) of the vertical displacement of the soil/structure point located in the first contact point between the rail and the soil/structure, induced by a unit force applied on the soil i-contact point between the rail and the soil/structure,

H_{rsnsi} is the Frequency Response Function (FRF) of the vertical displacement of the rail point located over the n-contact point connected to the soil/structure, induced by a unit force applied on the i-contact point between the rail and the soil/structure,

H_{snsi} is the Frequency Response Function (FRF) of the vertical displacement of the soil/structure point located in the n-contact point between the rail and the soil/structure, induced by a unit force applied on the soil i-contact point between the rail and the soil/structure.

It has to be highlighted that, for this specific example, a set of $n+2$ equations with $n+2$ unknowns is obtained. The unknowns are the $n+2$ vertical dynamic interaction forces (two at the wheel-rail interface and n at the rail-soil/structure level) that are derived once that the *Frequency Response Functions (FRF)* in terms of vertical displacement for the vehicle, the rail and the soil/structure in the examined $n+2$ contact points are known.

The vertical dynamic interaction forces so far obtained are expressed as analytic (complex) functions depending on the frequency and on the mechanical and inertial characteristics of vehicle, rail and underlying soils/structures. Furthermore, they are defined unless the rail defects (i.e. for a unit rail defect). If the mechanical behavior of whole system is linear and the rail defect are described by means of a PSD of the vertical displacements, the PSD of the dynamic vertical interaction force at the rail-soil/structure level in a specific connection point, i , can be derived by means of the following expression:

$$PSD_{F_{rsi}} = |F_{rsi}(f)|^2 \cdot PSD_{raildefect}(f) \quad (4)$$

where:

$PSD_{F_{rsi}}$ is the Power Spectral Density (PSD) function of vertical interaction force between the rail and the underlying soil/structure,

F_{rsi} is the Frequency Response Function (FRF) of the vertical interaction force between the rail and the underlying soil/structure at i -contact point for a unit rail defect,

$PSD_{raildefect}$ is the Power Spectral Density (PSD) function of rail defect,

and, in turn, under the superposition principle, the dynamic response of a arbitrary point, k , located in surrounding soils, expressed in terms of PSD of vertical displacement can be evaluated as:

$$PSD_{Dy,k} = \sum_{i=1}^n |FRF_{kFrSi}|^2 \cdot PSD_{F_{rsi}} = \sum_{i=1}^n |FRF_{kFrSi}|^2 \cdot |F_{rsi}(f)|^2 \cdot PSD_{raildefect}(f) \quad (5)$$

where:

$PSD_{Dy,k}$ is the Power Spectral Density (PSD) function of vertical displacement at point k ,

FRF_{kFrSi} is the Frequency Response Function (FRF) of the vertical displacement at point k induced by a unit vertical interaction force between the rail and the underlying soil/structure at i -contact point,

In order to simulate vibration level induced by the moving train, some considerations must to be made. As a matter of fact, if the rail defects can be represented by means of a stationary and ergodic random process, therefore vehicle oscillations and, in turn, dynamic forces are random stationary too if the dynamic system is linear. Therefore, assuming that the geometry of the problem is constant along the path of the moving force (i.e. the moving train), the dynamic response at a specific point of the surface induced by a moving vibration source can be evaluated by invoking the dynamic Betti-Rayleigh reciprocal theorem. According to this theorem, the response at a specific surface point, P , induced by a dynamic force moving along a defined path, is equal to the response induced by a fixed dynamic force along the path of an observer moving in parallel with the path of the force with the same velocity and passing through the point P [3, 12, 13].

On a operating point of view, once that the point, P , on which the dynamic response needs to be evaluated has been defined, PSD of dynamic response (i.e. vertical displacement) calculated through equation (5) for each point belonging to the path parallel to the train's path and passing through the point P is conveniently calculated. The overall amount of points along the path of the moving observer to be considered depends on the train velocity and on the time increment used in the numerical simulation. Then a Inverse Fourier Transform is carried out and a time history is derived for each point belonging to the moving observer path. The real time history of the point P can be therefore composed by extracting a single dynamic response value (i.e. the vertical displacement) from all the time histories evaluated so far when the moving observer passes through a specific point of the path on which the aforementioned time history has already been derived.

The main advantage of this approach is that it is not necessary to tackle the whole system (vehicle-rail-underlying soil/structure) but all the sub-models can be separately evaluated in order to extract the specific FRFs to be implemented in the set of equation described in (3), thus providing a dramatic decrease of the computational effort.

3. Application to a Case Study: Turin's Subway

3.1. Description of experimental site

The Turin's subway represents the first example of application in Italy of *Automatic Light Vehicle*, (*VAL*) system employing a rubber-tired vehicle. The VAL is designed so as to ensure maximum safety through a *Automatic Train Control* (*ATC*) system designed specifically for this type of vehicle that operates driverless. The latest generation of VAL, the 208 system, employs rubber-tyred vehicles running on steel plates. Guidance is provided by horizontally fitted tyres, in front of and behind the driving axles. The railway superstructure is a

ballastless track system with a H cross-section steel beam working as a rolling surface that is directly connected to the tunnel floor through a discrete resilient system employing a 1 m spaced rail pads. The layout of the rolling stock includes 2 permanent married cars. Each wagon is connected, through a suspension system, to four pneumatic tyres.

An experimental vibration monitoring campaign along Line 1 of the Turin's subway has been carried out within the VINCES Italian research project and it is detailed elsewhere [3]. The test site is located between the Rivoli and Racconigi stations, where the horizontal distance of the tunnel axis is about 20 m from the closest buildings (Figure 1). The site was selected because of the presence of a nearby downcast, which could facilitate the deployment of cables down to the tunnel, and the connection between the instruments installed along the line and the surface monitoring system.

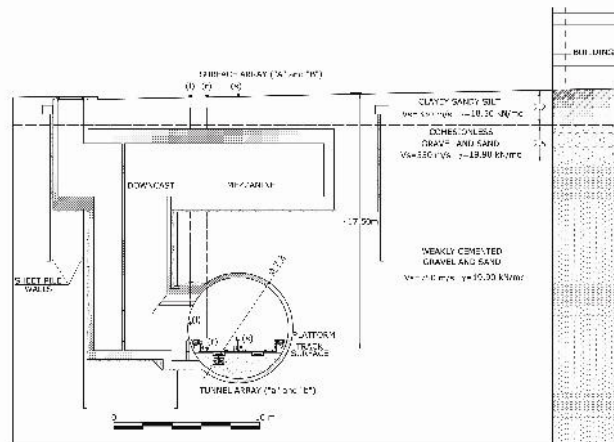


Fig. 1. Cross section view of the instrumented Turin test site.

The physical and mechanical properties of the subsoil were derived by geotechnical and geophysical reports for underground tunnel design supplied by Turin Transport Company following refraction and surface wave tests carried out by Turin Polytechnic [3]. The subsoil is characterized by stiff fluvial deposits of gravels and sands, weakly and randomly cemented that is overlaid by a cohesionless layer of sand and gravel; the uppermost layer is constituted by silt and sandy clay. Vibration measurements expressed in terms of vibration velocity have been carried out on two separate cross-sections 20m away from each other. It was therefore possible to derive train speed (~ 10 m/s) by analyzing the signal time lags. The sensors whose records were compared with vibration level provided by the prediction model were positioned at the center line of the section, close to the track and on the tunnel lining.

3.2. Characterization of generation and propagation models

Railway car has been modeled as a four degree-of-freedom lumped mass model comprising a vertical displacement for each of the two wheel axles and pitching and vertical displacement for the upper car body.

Mechanical and inertial parameters of the model have been derived from technical sheets or from scientific literature and are reported in the following table (see Table 1). It is worth to be noticed that since the wheel rail contact is between rubber and steel the Hertzian spring stiffness commonly adopted in the railway dynamics has been conveniently replaced by the tire vertical stiffness.

The rail superstructure was modeled as a Winkler beam resting on a continuous single layer of springs and dampers, whose relevant parameter are also reported in the Table 1. Frequency Response Functions derived from

the vehicle and the superstructure models have been conveniently evaluated in order to be introduced in the equation set (3). An overall amount of 40 discrete contact points at the rail-tunnel invert interface has been considered in the computations.

Since it was not possible to carry out direct measurement of rail defects on test site examined, the PSD of rail defects assumed in this study is that proposed by French Railways (SNFC) [2, 8]:

$$G_D(f) = \frac{G_D(\Omega)}{V} = \frac{A}{V(b + 2\pi \frac{f}{V})^3} \quad (6)$$

where:

$G_D(f)$ is the PSD of rail defects as a function of temporal frequency, in $m^2/(\text{cycles/s})$,

$G_D(\Omega)$ is the PSD of rail defects as a function of spatial frequency, in $m^2/(\text{cycles/m})$,

f is the temporal frequency of rail defects, in cycles/s,

Ω is the spatial frequency of rail defects in cycles/m,

A is a parameter dependent on the age of the track, (generally it is assumed $A = 1E-6$ or $2E-6$ for new and old railway tracks respectively),

b is equal to 0.36,

V is the train travelling speed, in m/s.

Table 1. Input parameters for vehicle and rail models

VEHICLE	
PARAMETER	Value
M_B , Car Body mass [kg]	15600
M_W , Wheel mass [kg]	250
K_S , Suspension vertical stiffness [N/m]	5.37×10^5
I_S , Suspension loss factor [-]	0.15
C_S , Suspension vertical viscous damping coefficient [Ns/m]	1.92×10^4
K_W , Tyre vertical stiffness [N/m]	1.1×10^6
n_W , Tyre loss factor [-]	0.06
V , Vehicle speed [m/s]	10
L , Vehicle wheel base [m]	10
A , parameter in SNCF roughness model [-]	1.0×10^{-6}
RAIL	
PARAMETER	Value
μ_R , Rail mass per unit length [kg/m]	63.134
I_R , Rail moment of inertia [m ⁴]	0.00002035
K_R , Rail vertical stiffness per unit length [N/m ²]	150×10^6
n_R , Rail pad loss factor [-]	0.07
C_R , Rail vertical damping coefficient per unit length [Ns/m ²]	1.3×10^4
i_R , Rail pad spacing [m]	1

A FEM approach has been chosen for the propagation model as the examined railway line is underground. The geometry and layout of the 3D FEM model were decided following a calibration phase and according to the stratigraphic characteristics of the test site. The considered study area extends 5m in radial direction, which corresponds to a uniform deposit of weakly cemented sand, and 10m in the longitudinal direction starting from a vertical symmetry plane. The study area examined was conveniently wrapped in both directions by means of a

surrounding damping area, which shows a gradual increase in the size of the mesh, in order to correctly simulate far field vibration propagation. As suggested in the technical literature, the mesh size was chosen in order to satisfy the following condition [14]:

$$d \leq \frac{\lambda_{\min}}{8} = \frac{V_S}{8 \cdot f_{\max}} \quad (7)$$

where:

d is the maximum finite element size,

λ_{\min} is the minimum wavelength,

V_S is the Shear Wave velocity of the surrounding soil,

f_{\max} is the maximum frequency of the Fourier spectrum.

The cylindrical surface was constrained in both radial and tangential directions, while constraints have been also placed on the plane of symmetry along the z-axis in order to fulfill the requirement of symmetry (see Figure 2). Mechanical properties of surrounding soils were derived from geotechnical and geophysical measurements whereas energy dissipation phenomena due to material damping were modelled through the Rayleigh approach. Finally, pulse vertical forces have been applied at tunnel invert level on the plane of symmetry in order to derive the Frequency Response Functions to be introduced in the equation set (3) previously described.

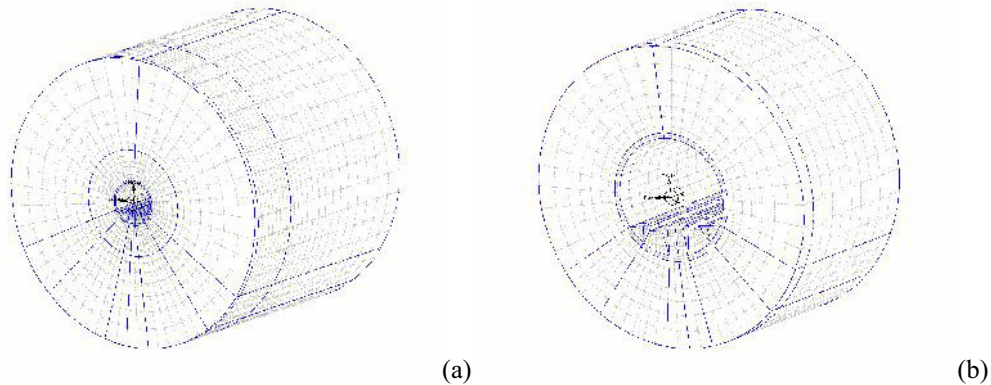


Fig. 2. 3D FEM model developed for the vibration propagation: general (a) and detailed (b) view..

4. Analysis of results

Results provided by numerical simulations have been compared with vibration level, expressed in terms of vertical velocity, measured by a sensor located on the tunnel invert close to the railway superstructure. A preliminary calibration of the model has been carried out in order to evaluate the influence of the rail defects level on the dynamic response since as previously mentioned, it was not possible to perform direct measurement of vertical track irregularity. Several simulations have been carried out by varying the scale parameter A already described in the equation (6). Results are reported in the following figure (Figure 3) in the time and frequency domain.

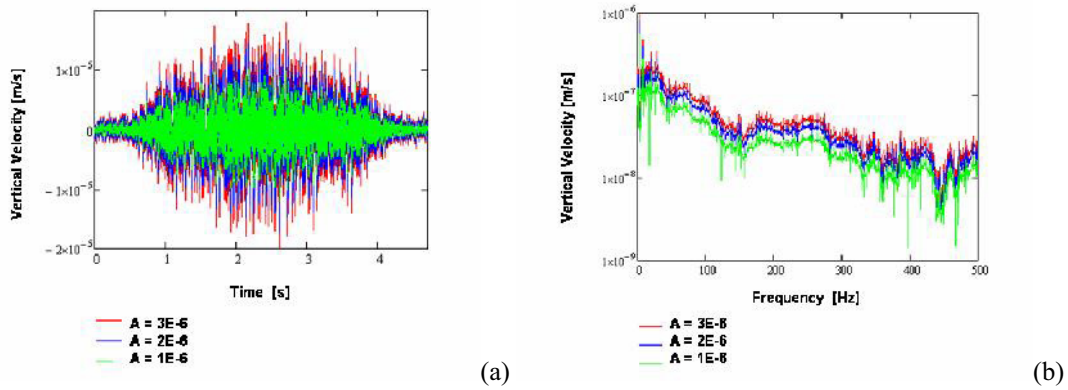


Fig. 3. Preliminary calibration of the prediction model: influence of rail defect level in the time (a) and frequency (b) domain.

As it can be observed in the figure, if the A parameter reported in the SNFC PSD of rail defects is increased, a significant amplification of the vibration amplitude can be detected in time domain. This corresponds to a vertical shift of the modulus of response spectrum in the frequency domain.

Following these results, an A value of $1E-6$, as suggested for new railway tracks, has been assumed. Comparison in terms of vertical vibration velocity between the dynamic response provided by the model and the vibration level measured on the test site is depicted in the following figure (Figure 4).

As it can be seen from the figure, the comparison has showed a good agreement between numerical and experimental data with regard to the maximum amplitudes of vibration velocity in the time domain. As far as the comparison in the frequency domain is concerned, numerical and experimental velocity spectra show a fairly good agreement up to 300 Hz, that it can be considered a satisfying frequency range of interest for the prediction of ground-borne vibration induced by railway traffic.

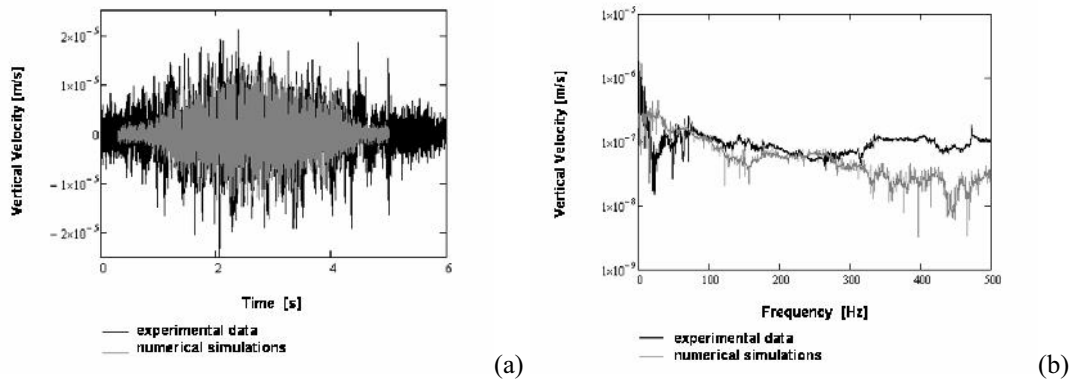


Fig. 4. Comparison of dynamic response between the experimental data and the numerical simulations in the time (a) and frequency (b) domain.

5. Conclusions

In this paper, a methodology to estimate the level of vibration induced by railway traffic has been proposed. The method takes into account the dynamic interaction of all the systems involved: vehicle, superstructure and

surrounding/underlying soils/structures. The method has been applied to a case study located in the Turin's subway where an extensive vibration monitoring experimental campaign has been carried out within a recent National Research Project. The vehicle and superstructure were modelled as discrete lumped mass system and as a Winkler beam resting on a continuous visco-elastic support respectively. A PSD of rail defects proposed by French Railway Company has been employed. In order to take into account of the effective stiffness offered by the tunnel-soil system a FEM based propagation model has been developed, whose results in terms of frequency response functions were used to calculate the dynamic interaction forces between the superstructure and the tunnel invert.

The results provided by the mathematical model developed so far were compared with some experimental measurements carried out on the Turin's subway test site and the proposed methodology seems to provide fairly satisfactory results as regards the comparison in both time and frequency domain.

A better model calibration and agreement with experimental data could have been obtained if direct measurements of rail defects were performed on the test site since excitations have actually been derived from models proposed in the technical literature.

Acknowledgements

Prof. Francesco Silvestri of University of Naples "Federico II" and Prof. Laura Valentina Socco of Turin Polytechnic, Eng. Vincenzo Aiello, Dott. Daniele Boiero are gratefully acknowledged for providing the experimental data and for their suggestions and encouragements.

References

- [1] D'Apuzzo, M., & Nicolosi, V. (2003). "Evaluation of pavement-oriented countermeasures to mitigate traffic induced vibrations in urban areas". 5th European Conference on Noise Control: EURONOISE 2003, May 19th-22nd 2003, Naples, Italy, 1-6.
- [2] Crispino, M., D'Apuzzo, M., & Lamberti, R. (2003). "Development and experimental validation of a prediction model to assess railway induced vibrations". 5th European Conference on Noise Control: EURONOISE 2003, May 19th-22nd 2003, Naples, Italy, 1-6.
- [3] Aiello, V., Boiero, D., D'Apuzzo, M., Silvestri, F., & Socco, V. (2008). "Experimental and numerical analysis of vibrations induced by underground trains in urban environment". *Journal of Structural Control and Health Monitoring*, Vol. 15, DOI: 10.1002/stc.247, Wiley InterScience, 315-348.
- [4] Esveld, C. (2001). *Modern railway track: second edition*, MRT-Productions, Zaltbommel, The Netherlands; 1-654.
- [5] Iwnicki, S. (2006). *Handbook of railway vehicle dynamics*, CRC Press, Boca-Raton, Florida, 1-526.
- [6] Wu, T.X., & Thompson, D.J. (2000). "Theoretical investigation of wheel/rail non-linear interaction due to roughness excitation", *Vehicle System Dynamics*, (34), 261-282.
- [7] DeGrande, et al. (2006). "A numerical model for ground-borne vibrations from underground railway traffic based on a periodic finite element-boundary element formulation", *Journal of Sound and Vibration*, (293), 645-666.
- [8] Alias, J. (1977). *La Voie Ferrée*, Collections des Chemins de Fer, Eyrolles Editeur, Paris, 1-472.
- [9] Cox S.J., & Wang, A. (2003). "Effect of track stiffness on vibration levels in railway tunnels", *Journal of Sound and Vibration*, (267), 565-573.
- [10] Gardien, W., & Stuit, H.G. (2003), "Modelling of soil vibrations from railway tunnels", *Journal of Sound and Vibration*, (267), 605-619.
- [11] Andersen, L., & Jones, C.J.C. (2006). "Coupled boundary and finite element analysis of vibration from railway tunnels – a comparison of two- and three-dimensional models", *Journal of Sound and Vibration*, (293), 611-625.
- [12] Lombaert, G., & De Grande, G. (2001). "Experimental validation of a numerical prediction model for free field traffic induced vibrations by in situ experiments", *Soil Dynamics and Earthquake Engineering*, Elsevier Science, 21, 485-497.
- [13] D'Apuzzo, M. (2007). "Some remarks on the prediction of road traffic induced ground-borne vibrations". *Proceedings of the 4th International SIV Congress*. Palermo. 12th-14th September 2007, GRAFILL S.r.l., 1-13.
- [14] Lysmer, J., & Kuhlemeyer, L. (1969). "Finite dynamic model for infinite media", *ASCE Journal of the Engineering Mechanics Division*, (95), 859-877.